1999-03

Huygens-Fresnel wave-optics simulation of atmospheric optical turbulence and reflective speckle in CO2 differential absorption LIDAR (DIAL)

Nelson, Douglas H.; Petrin, Roger R.; MacKerrow, Edward P.; Schmitt, Mark J.; Foy, Bernard R.; Koskelo, Aaron C.; McVey, Brian D.; Quick, Charles R.; Porch, William M.; Tiee, Joe J....

Los Alamos, New Mexico. Los Alamos National Laboratory

D.H. Nelson, et al., "Huygens-Fresnel wave-optics simulation of atmospheric optical turbulence and reflective speckle in CO2 differential absorption LIDAR (DIAL)," ITR Conference, March 23-25, 1999, 14 p.
http://hdl.handle.net/10945/52710

LA-UR- 99-2271

Approved for public release; distribution is unlimited.

Title: HUYGENS-FRESNEL WAVE-OPTICS SIMULATION OF ATMOSPHERIC OPTICAL TURBULENCE AND REFLECTIVE SPECKLE IN CO2 DIFFERENTIAL ABSORPTION LIDAR (DIAL)

Author(s): D. H. NELSON
R. R. PETRIN
E. P. MACKERROW
M. J. SCHMITT
B. R. FOY
A. C. KOSKELO
B. D. MCVEY
et. al.

Submitted to: ITR CONF.
MARCH 23-25, 1999

Los Alamos
NATIONAL LABORATORY

DISCLAIMER

Huygens-Fresnel wave-optics simulation of atmospheric optical turbulence and reflective speckle in CO_2 differential absorption lidar (DIAL)

Douglas H. Nelson[a], Roger R. Petrin[a], Edward P. MacKerrow[a], Mark J. Schmitt[a], Bernard R. Foy[a], Aaron C. Koskelo[b], Brian D. McVey[a], Charles R. Quick[b], William M. Porch[c], Joe J. Tiee[a], Charles B. Fite[d], Frank A. Archuleta[a], Michael C. Whitehead[e] and Donald L. Walters[f]

[a]Los Alamos National Laboratory, MS E543, Los Alamos, NM 87545
[b]Los Alamos National Laboratory, MS J565, Los Alamos, NM 87545
[c]Los Alamos National Laboratory, MS D407, Los Alamos, NM 87545
[d]Los Alamos National Laboratory, MS D440, Los Alamos, NM 87545
[e]Los Alamos National Laboratory, MS J567, Los Alamos, NM 87545
[f]Naval Postgraduate School, Code PH/We, Monterey, CA 93943

ABSTRACT

The measurement sensitivity of CO_2 differential absorption lidar (DIAL) can be affected by a number of different processes. We have previously developed a Huygens-Fresnel wave optics propagation code to simulate the effects of two of these processes: effects caused by beam propagation through atmospheric optical turbulence and effects caused by reflective speckle. Atmospheric optical turbulence affects the beam distribution of energy and phase on target. These effects include beam spreading, beam wander and scintillation which can result in increased shot-to-shot signal noise. In addition, reflective speckle alone has been shown to have a major impact on the sensitivity of CO_2 DIAL. However, in real DIAL systems it is a combination of these phenomena, the interaction of atmospheric optical turbulence and reflective speckle, that influences the results. In this work, we briefly review a description of our model including the limitations along with previous simulations of individual effects. The performance of our modified code with respect to experimental measurements affected by atmospheric optical turbulence and reflective speckle is examined. The results of computer simulations are directly compared with lidar measurements and show good agreement. In addition, advanced studies have been performed to demonstrate the utility of our model in assessing the effects for different lidar geometries on RMS noise and correlation "size" in the receiver plane.

Keywords: atmospheric turbulence, laser speckle, beam propagation

1. INTRODUCTION

The measurement sensitivity of CO_2 differential absorption lidar (DIAL) can be affected by a number of different processes. Two of these processes are atmospheric optical turbulence and reflective speckle. Atmospheric optical turbulence affects the spatial distribution of energy and phase. Measurable effects include beam spreading, beam wander and scintillation which can result in increased shot-to-shot signal noise. In addition, reflective speckle alone has been shown to have a major impact on the sensitivity of CO_2 DIAL.

The geometry of a hard target reflection scheme is shown in Figure 1. As the laser beam propagates toward the target, index of refraction fluctuations in the atmosphere cause phase distortions in the transverse electric field distribution. Once the laser beam reaches the target, its spatial intensity distribution has been altered compared to what would be observed in propagating through a vacuum. At the target, light is scattered back toward the transmitter. This light passes through essentially the same turbulent atmosphere that altered the outgoing beam (since the atmosphere is "frozen" during the transit time of the pulse for our typical lidar geometries). The return signal will be reduced by any absorbing species in the path in accordance with Beer's law. Absorption will also occur from normal atmospheric constituents.

We have developed a Huygens-Fresnel wave optics propagation code to simulate the effects of reflective speckle and atmospheric optical turbulence. Previously, we compared the ability of our model to predict these separate effects with a combination of theory and experimental observations. [1,2] However, in real DIAL systems it is a combination of these

phenomena, the interaction of atmospheric optical turbulence and reflective speckle, which influences the results.[3] We present preliminary results of the comparison of our combined effects simulation with experimental measurements over a finite aperture. We have begun advanced studies to determine the nature of the reflective speckle-atmospheric turbulence interaction and provide some of our findings thus far.

2. MODEL

The model employs the Fresnel-Kirchoff theorem with the Fresnel approximation and assumes paraxial, on-axis propagation.[4,5] The atmospheric optical turbulence effects are approximated by a series of phase screens over several propagation steps.[6,7] This model is applied to a lidar geometry in which the beam propagates from the transmitter/receiver through an optically turbulent atmosphere to a diffuse hard target. To simulate reflection from a diffuse hard target, we randomize the phase. After scattering from the target, the portion of the beam that reflects back to our receiver propagates along the same optically turbulent path.

Our Huygens-Fresnel wave optics simulation uses an N x N array of complex numbers to represent the electric field in a plane perpendicular to the propagation axis. The initial electric field, a Gaussian TEM_{00} spatial intensity and phase distribution with the properties of our experimental transmitter beam, is used as the input for the simulation. The simulation propagates this initial electric field by dividing the path from lidar system to the target into equal sized steps and applying a phase screen to simulate turbulence effects at each step. The expression for the electric field after a step of distance Δz is determined from[7]

$$E(\hat{\rho},\Delta z)=IFT\left[\exp\left(i\cdot\pi\cdot\lambda\cdot\Delta z\cdot\left|\hat{f}\right|^2\right)\cdot FT\left[E(\hat{\rho},0)\cdot\exp\{i\cdot\theta(\hat{\rho})\}\right]\right], \quad (1)$$

where $E(\hat{\rho},0)$ is the electric field at the initial portion of the step ($z=0$) with the transverse coordinate given by $\hat{\rho}$. FT is the discrete two-dimensional Fourier transform, $\exp\left(i\cdot\pi\cdot\lambda\cdot\Delta z\cdot\left|\hat{f}\right|^2\right)$ is the Fresnel propagator in the spatial frequency domain $\hat{f}$, λ is the laser wavelength and IFT is the discrete two-dimensional *inverse* Fourier transform. The phase screen, $\theta(\hat{\rho})$, is[6,7]

$$\theta(\hat{\rho})=0.0984\cdot k_o\cdot\sqrt{C_n^2(z)\cdot\Delta z}\cdot(N\cdot\delta x)^{5/6}FT\left[\left(\sqrt{n_x^2+n_y^2}\right)^{-11/6}\cdot\Theta_o(n_x,n_y)\right], \quad (2)$$

where $k_o=2\pi/\lambda$, $C_n^2(z)$ is the path dependent index of refraction structure constant which characterizes the level of turbulence[8], Δz is again the step propagation distance, N is the number of pixels along one dimension of the transverse array, $\delta x=\sqrt{\lambda L/N}$ is the optimized pixel width for a transmitter-to-hard target distance of L, n_x and n_y denote integer pixel coordinates within the two-dimensional transverse array, $\Theta_o(n_x,n_y)$ represents an N x N array of complex unit-variance Gaussian random numbers and FT again implies the two-dimensional discrete Fourier transform. The argument of the FT operation is an array in the spatial frequency domain produced by taking a Gaussian random number distribution and applying the $\left(\sqrt{n_x^2+n_y^2}\right)^{-11/6}$ factor to impose properties of the Kolmogorov spectrum, which describes the spatial frequency distribution of index of refraction fluctuations, in the transverse plane.[9] As seen in Equation (2), the magnitude of the turbulence induced phase is dependent on the strength of the turbulence, the length of the propagation step and the lidar wavelength.

The number of propagation steps has a direct impact on computation time. To keep this computation time at a minimum, one goal is to keep the number of propagation steps as low as possible. However, our model is limited in that there are constraints on propagation step size. The assumptions used to approximate a propagation step dictate that the step be within the near field propagation distance. For our lidar geometry, this means that the step can be no longer than the Rayleigh range of our laser transmitter.

Another constraint is that phase effects over this step must not be dominated by amplitude effects. Martin and Flatté [10] found that for the phase screen approach to be valid, the normalized point irradiance, $\sigma_{\bar{I}}^2$, defined below, for a single propagation step must be less than $1/10$ of the total normalized point irradiance variance for the total propagation distance, L,

$$\sigma_{\bar{I}}^2(\Delta z) < 0.1\sigma_{\bar{I}}^2(L). \quad (3)$$

In addition, they found that this variance must be less than 0.1 for one step

$$\sigma_{\bar{I}}^2(\Delta z) < 0.1. \quad (4)$$

For spherical wave propagation, assuming weak turbulence, the RMS noise or scintillation at an on-axis point detector is[11]

$$\sigma_{\bar{I}} = \sqrt{\exp(4\sigma_\chi^2) - 1}, \quad (5)$$

where $\sigma_{\bar{I}} = \sigma_I / \bar{I}$ is the normalized standard deviation of irradiance. This is the square root of the normalized point irradiance variance discussed earlier. The value σ_χ^2 is the spherical wave log amplitude variance for a point detector. For a path of length L with uniform turbulence along the entire path (i.e. constant turbulence level - C_n^2) the spherical wave log amplitude variance is[8]

$$\sigma_\chi^2 = 0.124 C_n^2 k_o^{7/6} L^{11/6}, \quad (6)$$

again with $k_o = 2\pi/\lambda$.

3. SIMULATION OF INDIVIDUAL EFFECTS

We have shown that this model works well predicting separately the effects of atmospheric optical turbulence and reflective speckle.[1,2] The simulation of long-term turbulent beam spreading was found to be in agreement with both experimental data and analytical predictions. Simulation values for point detector scintillation due to atmospheric optical turbulence showed agreement with analytical predictions. This last comparison is provided in Figure 2 as an example of our previous work.

We also considered separately the reflective speckle effects in the absence of atmospheric optical turbulence.[1,2] A surface that is rough on the scale of the laser wavelength scatters the coherent lidar pulse, which produces a complex interference pattern.[12] This pattern is granular in appearance and is commonly referred to as a speckle pattern. Simulated speckle coherence or correlation "sizes" were found to be in excellent agreement with those predicted by theory. The intensity probability distributions predicted by our simulation for circular receiver apertures of varying radii agreed with those observed in experiment and expected from theory. These probability distributions are characterized by the parameter *M*, which is interpreted as the number of speckle inside the receiver for an average pulse. We compared these *M* values to geometrical predictions from the ratio of the receiver aperture area to the estimated speckle correlation area. We also compared the *M* values from these probability distributions to the signal-to-noise ratio obtained from the simulation. These comparisons are presented in Figure 3 and Figure 4 as examples of the resulting excellent agreement between the simulation and theoretical predictions. The simulated intensity probability distributions were consistent with those measured experimentally.[13]

4. COMBINED EFFECTS SIMULATION AND COMPARISON WITH EXPERIMENT

We conducted experiments during June and July 1998 in the Nevada desert under conditions of diurnally varying levels of atmospheric turbulence (C_n^2) at ranges of ~1350 m and ~2150 m. The target at ~1350 m was a rotating drum with a diffuse surface. This rotating drum was specifically designed to provide independent speckle realizations as the drum turns at ~ 2 revolutions per minute. The target at ~2150 m had a diffuse surface fixed to plywood. Our lidar consisted of a CO_2 laser with an effective pulse rate per line of ~113 Hz. The receiver configuration was annular with an inner diameter of ~ 4.5" and an outer diameter of ~ 12". The propagation path was horizontal over flat, featureless desert terrain. We concurrently measured the turbulence level with an incoherent near infrared scintillometer propagating over a path that was approximately parallel azimuthally to our lidar beam but on a slant path at a different height.[14] In determining effective turbulence levels for the experiment, we took these differences in the paths into account.[8]

The simulation employed a 1024 x 1024 array and five propagation steps. A total of 100 realizations were run for each turbulence level. The signal was integrated over an annulus that was the same size and configuration as our experimental receiver. Independent speckle realizations were modeled in addition to independent turbulence realizations. The turbulence level (C_n^2) was simulated as uniform over the propagation path.

The model predictions for the combined effects on single-shot RMS noise and comparison to experimental results appear in Figure 5 and Figure 6 for the two ranges mentioned above. The two laser lines we used for this experimental comparison were chosen because of their negligible atmospheric absorption under normal operating conditions. The model, which neglects atmospheric absorption, accurately predicts the level of single-shot RMS noise for our annular aperture. It also correctly predicts the trend of increasing noise with increasing C_n^2.

5. ADVANCED STUDIES

We have begun advanced studies to learn more about the reflective speckle-atmospheric turbulence interaction. In practice, there are lidar geometries in which the turbulence is not uniform along the entire propagation path. These studies also serve to illustrate the utility of our model.

A. Correlation Size in the Receiver Plane

An example of these studies, in which we investigate the impact of cases of uniform/non-uniform turbulence on the correlation diameter in the receiver plane, is shown in Figure 7 and Figure 8. The simulation consisted of 100 realizations of atmospheric turbulence and reflective speckle for each specific case, which will be discussed below, using a 512 x 512 grid. The 2000 m propagation path was divided into five 400 m steps. The normalized autocovariance of the speckle intensity at the receiver was determined for each realization and a Gaussian curve was fit to each to determine the correlation diameter.[1] The mean and standard deviation of the 100 Gaussian curve fits was retrieved for each case and is depicted in the figures. The beam divergence input to the simulation was ~200 μrad resulting in a relatively large correlation diameter (~6.61 $\pm$ 0.01 cm) for the zero turbulence case.

It should be pointed out that the Gaussian fit of the normalized autocovariance of the speckle intensity strictly applies to the case of a Gaussian TEM_{00} beam scattered at the diffuse target.[12,13] In the case of turbulence along the outgoing portion of the propagation path, the beam on target will not be perfectly Gaussian. However, for the weak levels of turbulence we examine, the deviation from the vacuum case is minimal and provides a semi-quantitative insight into the relative effects of turbulence for the cases we explore. We use the term correlation size to describe a pattern that has been affected by atmospheric turbulence. The term speckle correlation size refers strictly to the case of propagation through vacuum or zero turbulence.

In Figure 7 we consider two cases in comparison with the vacuum case (Zero Turbulence). In one case, turbulence is present along the entire propagation path (All Phase Screens Round Trip). Here, the correlation diameter is smaller than the speckle correlation diameter in the vacuum case. We also consider the weighting effect of turbulence contained in only one propagation step for both the outgoing and return legs of the path (Phase Screen Weight Round Trip). The effect here is greatest near the center of the propagation path where the smallest correlation diameters occur. For the portion of the path nearest the target, the effect is negligible since the target will provide randomization that will far outweigh the effects of the phase screen. The phase screen for the step shown in Figure 7 and Figure 8 has a phase standard deviation of ~0.2π radians with maximum phase variations of ~0.6π radians. The target phase randomization is uniformly distributed between 0 and 2π radians.

We examine in Figure 8 the weighting effect for the cases of turbulence contained in one step on: (1) the outgoing path (Phase Screen Weight Out) and (2) the return path (Phase Screen Weight Back). For the outgoing path case (Phase Screen Weight Out), the return path had zero turbulence. Likewise, for the return path case (Phase Screen Weight Back), the outgoing path had zero turbulence. In the case of the outgoing path (Phase Screen Weight Out), this effect is minimal and result in correlation diameters very close to the value of the speckle correlation diameter found in the vacuum case (Zero Turbulence). By contrast, the weighting effect of one step on the return path (Phase Screen Weight Back) is similar to our round trip weighting results (All Phase Screens Round Trip) of Figure 7.

We also found that uniform turbulence along the entire outgoing path with a return propagation through vacuum resulted in a correlation diameter that is very close to our vacuum value. On the other hand, turbulence along the entire return path after

an outgoing propagation in vacuum resulted in a value very close to the full turbulence case (All Phase Screens Round Trip) depicted in Figure 7. Hence, turbulence on the return path has the greater effect on the reduction of speckle correlation size.

B. RMS Noise

When compared to the case of speckle correlation size, we see a different relative effect of turbulence on the normalized standard deviation of intensity or RMS noise, as shown in Figure 9. The simulation consisted of 1000 realizations of atmospheric turbulence and reflective speckle for each specific case using a 512 x 512 grid. As before, the 2000 m propagation path was divided into five 400 m steps. However, the turbulence level is an order of magnitude higher than in the case of speckle correlation size.

There is a definite increase in the level of single-shot RMS noise over the zero turbulence case. The atmospheric turbulence near the target has a greater effect on increasing RMS noise than any other portion of the propagation path. For turbulence along the entire round-trip path, we found an increase in RMS noise that was only slightly higher than the level shown for the case of turbulence on just the propagation step near the target.

Assuming that the reduction of speckle correlation size occurs for the higher turbulence level modeled in this RMS noise case, it is not a dominant factor in determining the RMS noise. According to accepted speckle theory, smaller speckle correlation sizes should result in lower noise. However, we see an increase in RMS noise in Figure 9. There is obviously another effect besides reduction of correlation diameter driving the resulting increase in RMS noise. Further study will be required to determine the true nature of this RMS noise increase. Reduction of correlation diameter may be limiting the increase in RMS noise but it does not mitigate it entirely.

6. CONCLUSIONS

For the lidar geometry of our experiment, the single-shot RMS noise is 40-50% larger under the higher turbulence conditions. The impact of this trend for lidar operations is significant. Even if multi-shot averaging is used to improve the lidar measurement, the initial noise level will be markedly higher for conditions of increased turbulence.

Our model accurately predicted the level of RMS noise for our finite aperture. It also predicted the trend of increasing RMS noise with increasing turbulence level (C_n^2) for our lidar geometry.

These results provide experimental verification for our modeling of the combined effects of atmospheric optical turbulence and reflective speckle. The results also emphasize, for this lidar geometry, the impact of increased turbulence levels on lidar operations and provide motivation for further study.

The study of the relative effects of turbulence on correlation diameter in the receiver plane provides some insight into the reflective speckle-atmospheric turbulence interaction. One finding is that the turbulence on the return path from the target has a much greater impact on reducing the size of relatively large speckle than turbulence on the outgoing path. We also found that the turbulence near the center of the return path has the greatest effect on the reduction of correlation size. The effect of turbulence near the target had almost no impact on reducing the relatively large correlation diameter.

Turbulence only near the target, however, produced a greater increase in RMS noise, over the vacuum case, than any other portion of the propagation path. In fact, the increase in RMS noise for turbulence only near the target was nearly as great as that seen for turbulence along the entire propagation path. The implication for lidar systems is clear. If the atmospheric turbulence near the transmitter/receiver is low, turbulence near the target by itself will increase the RMS noise of the measurement. Reduction of correlation size, discussed above, is obviously not a dominant factor in determining the level of RMS noise. There may be a partial mitigation of the increase in RMS noise because of an increase in the number of correlation areas collected by the receiver telescope but no overall decrease as one would expect from established speckle theory.

Our advanced studies have thus far involved weak turbulence regimes for the study of speckle correlation size reduction and moderate to strong levels for the study of RMS noise. Future work will include further quantification of the model's limitations so that stronger turbulence values may be used.

ACKNOWLEDGEMENTS

This work was part of a large lidar project with many important team members and we wish to thank all of them. In particular we thank L. John Jolin for his contributions to this research. The authors would also like to acknowledge the cooperation of the Nevada Test Site Spill Test Facility, the DOE Remote Sensing Laboratory, Nellis Air Force Base and Air Force Research Laboratory. We are very grateful to the project leader, John F. Schultz, who directed this research. This research was fully supported by the U.S. Department of Energy under contract W-7405-ENG-36.

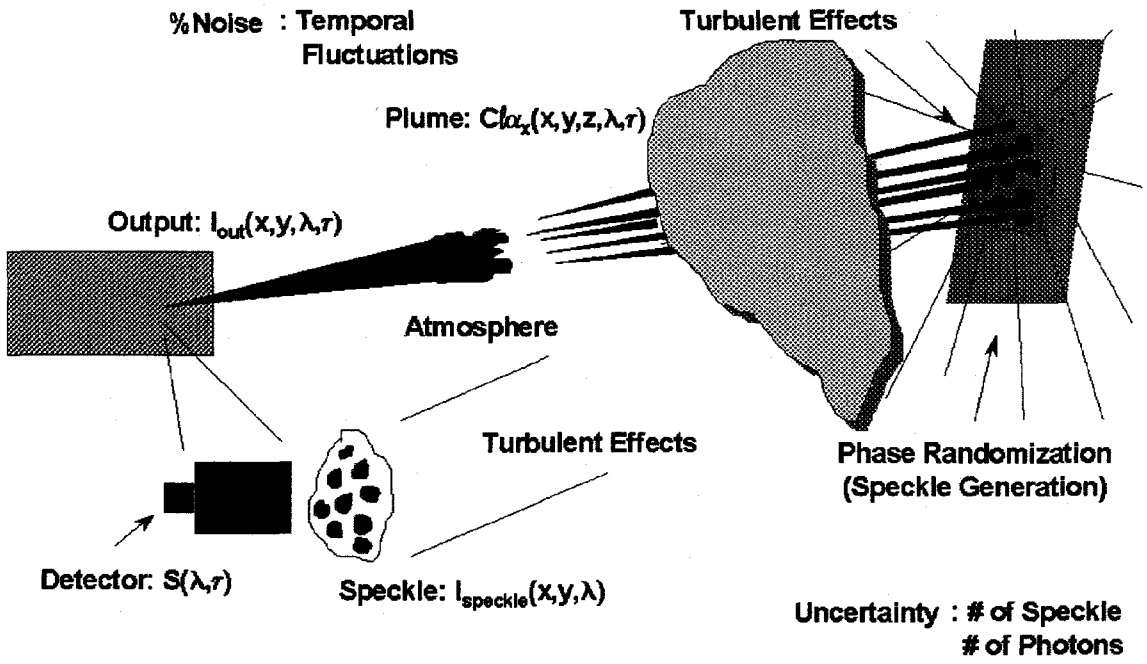

Figure 1. Hard target reflection scheme of lidar highlighting effects of the atmosphere and the target on the return signal.

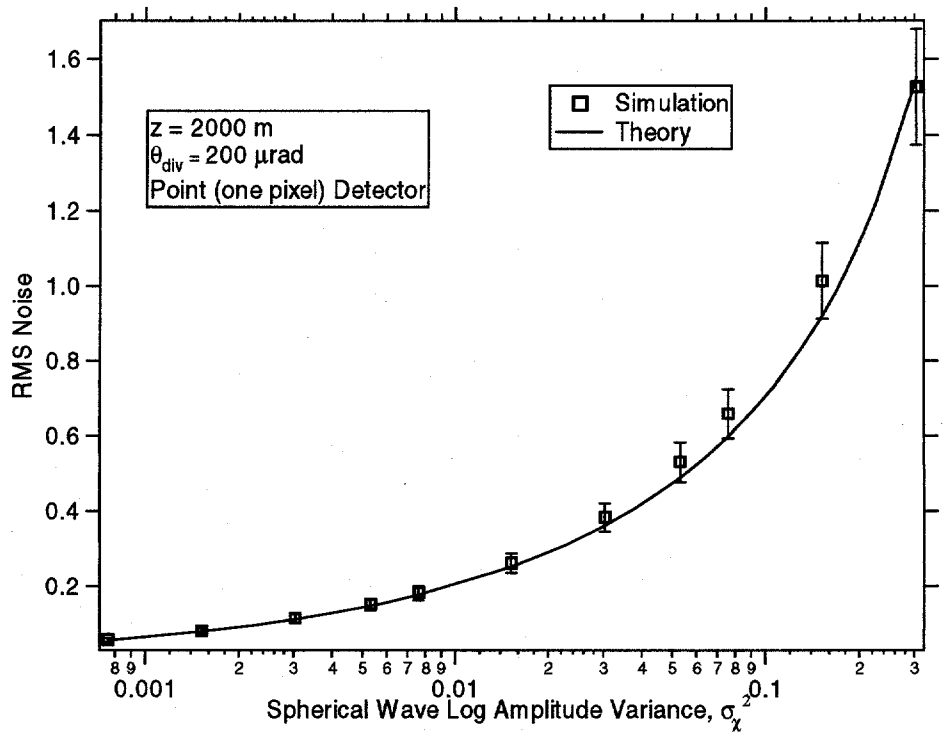

Figure 2. Scintillation of a lidar beam for a point (one pixel ~ 0.0046 m x 0.0046 m square) receiver after a 2000 m round trip propagation assuming no reflective speckle generation. The beam divergence is 200 μrad and the laser wavelength is 10.6 μm.

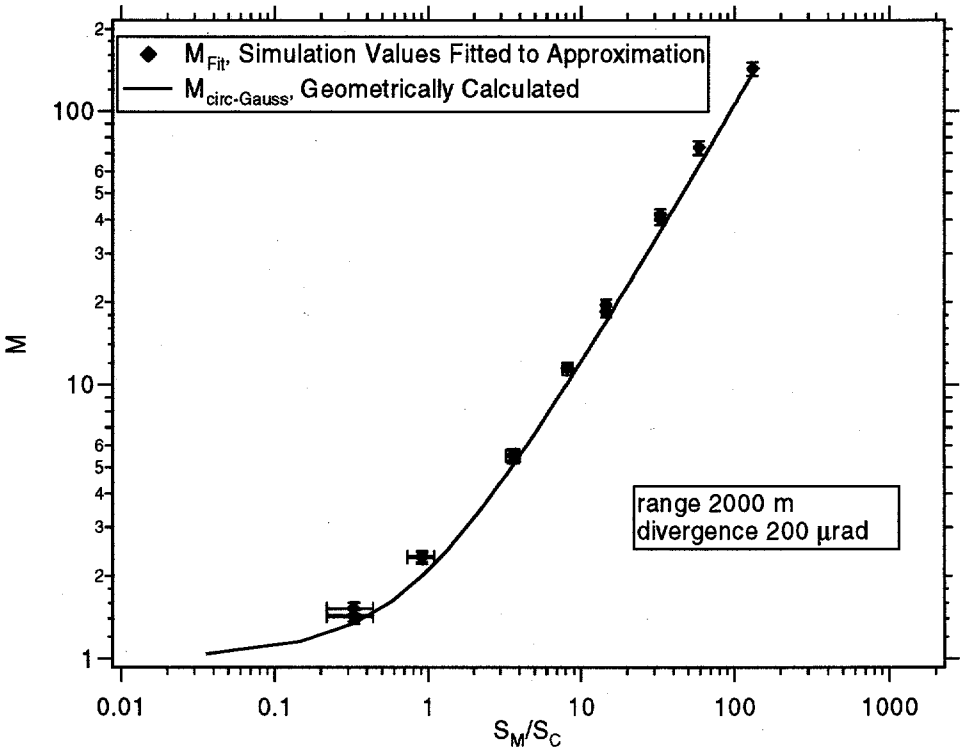

Figure 3. *M* values compared with receiver area/speckle "area" ratio for 1000 pulse intensity probability distributions and a 2000 m one way propagation with independent speckle realizations. Five propagation steps were used for each leg of the round trip with a 512 x 512 grid, a beam divergence of 200 μrad and a laser wavelength of 10.6 μm.

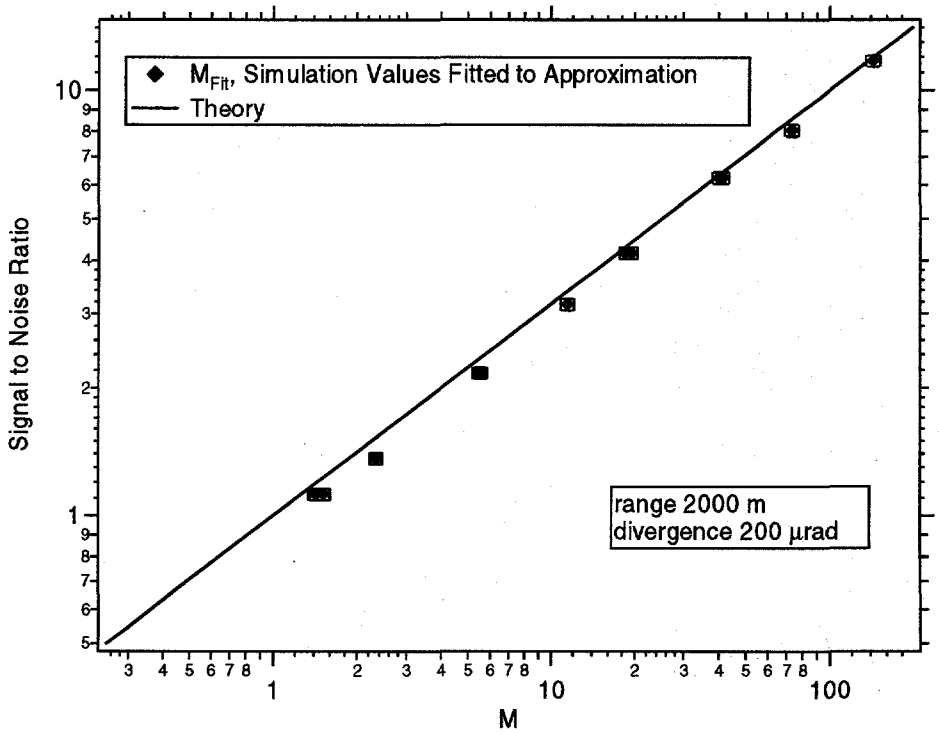

Figure 4. Signal-to-noise ratio versus M for 1000 pulse intensity probability distributions and a 2000 m one way propagation with independent speckle realizations. Five propagation steps were used for each leg of the round trip with a 512 x 512 grid, a beam divergence of 200 µrad and a laser wavelength of 10.6 µm.

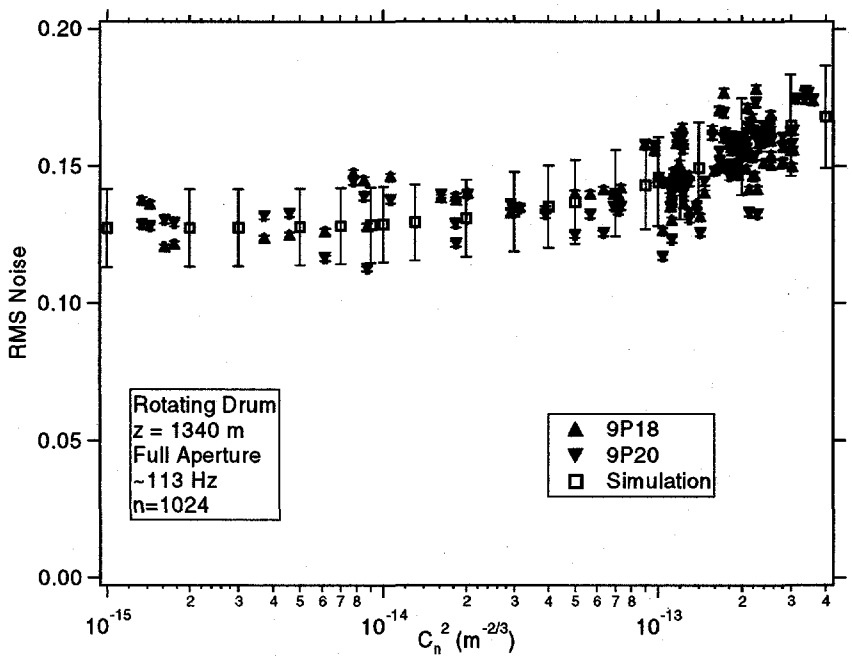

Figure 5. Comparison of simulation with experiment for a target at ~1340 m. The beam divergence was approximated as ~340 µrad. The receiver is annular with an area of ~ 0.06 m^2. The simulation grid was 1024 x 1024. Five propagation steps were used for each leg of the round trip path. The propagation path was assumed horizontal with a uniform turbulence level along the path.

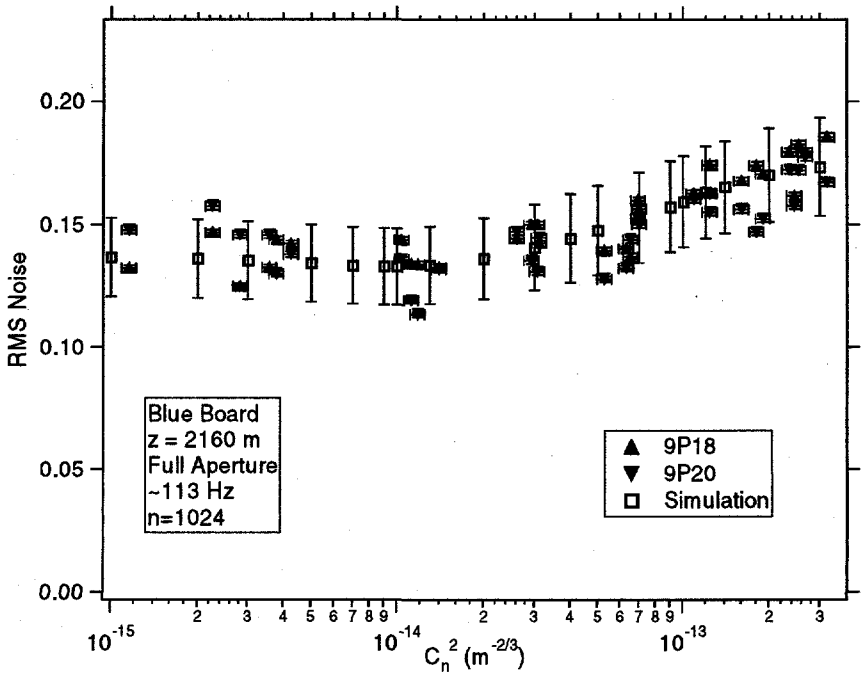

Figure 6. Comparison of simulation with experiment for a target at ~2160 m. The beam divergence was approximated as ~340 μrad. The receiver is annular with an area of ~ 0.06 m^2. The simulation grid was 1024 x 1024. Five propagation steps were used for each leg of the round trip path. The propagation path was assumed horizontal with a uniform turbulence level along the path.

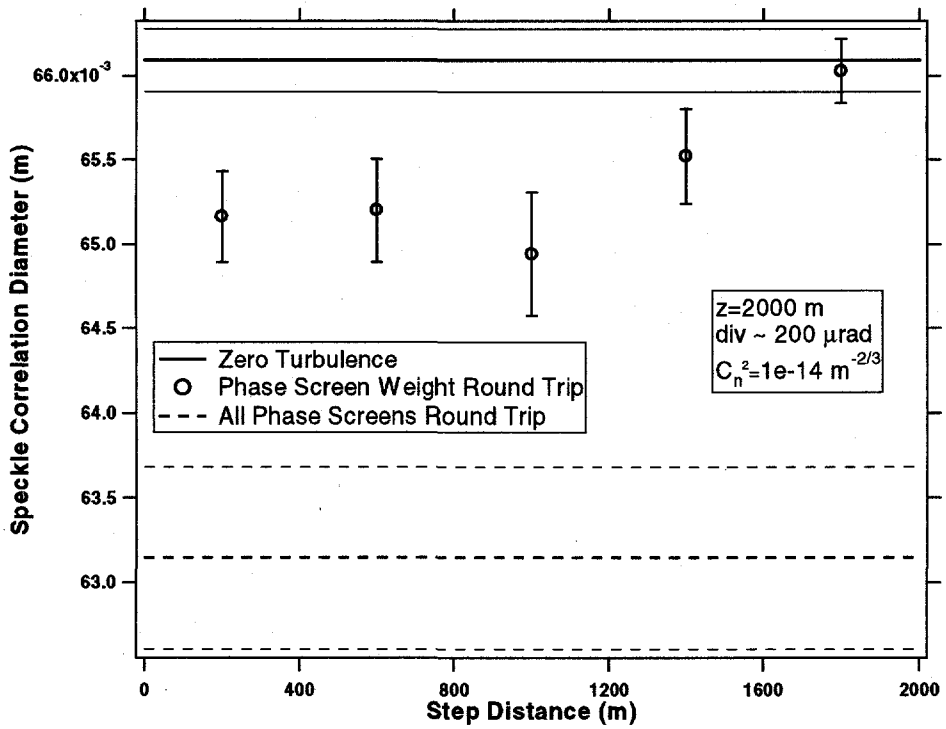

Figure 7. A comparison of the weighting effect of turbulence along the propagation path on correlation diameter. The solid lines depict the mean and standard deviation for the vacuum case (Zero Turbulence). The dashed lines (All Phase Screens Round Trip) indicate the mean and standard deviation for the case in which there is turbulence in both the outgoing and return portion of the entire propagation path. The circles (Phase Screen Weight Round Trip) indicate the case in which turbulence exists on the outgoing and return portions of only one propagation step (400 m).

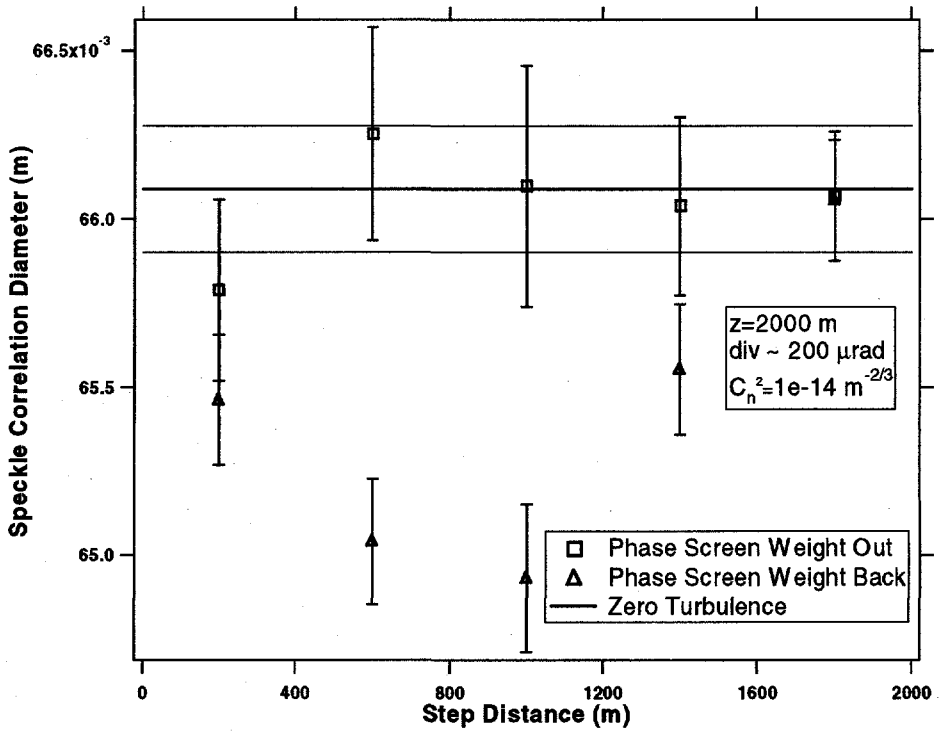

Figure 8. The effect of outgoing/return weighting of turbulence along the propagation path on the correlation diameter. The solid lines depict the mean and standard deviation for the vacuum case (Zero Turbulence) as in Figure 7. The squares (Phase Screen Weight Out) indicate the case in which turbulence exists only on the outgoing portion of one propagation step (400 m). The triangles (Phase Screen Weight Back) indicate the case in which turbulence exists only on the return portion of one propagation step (400 m).

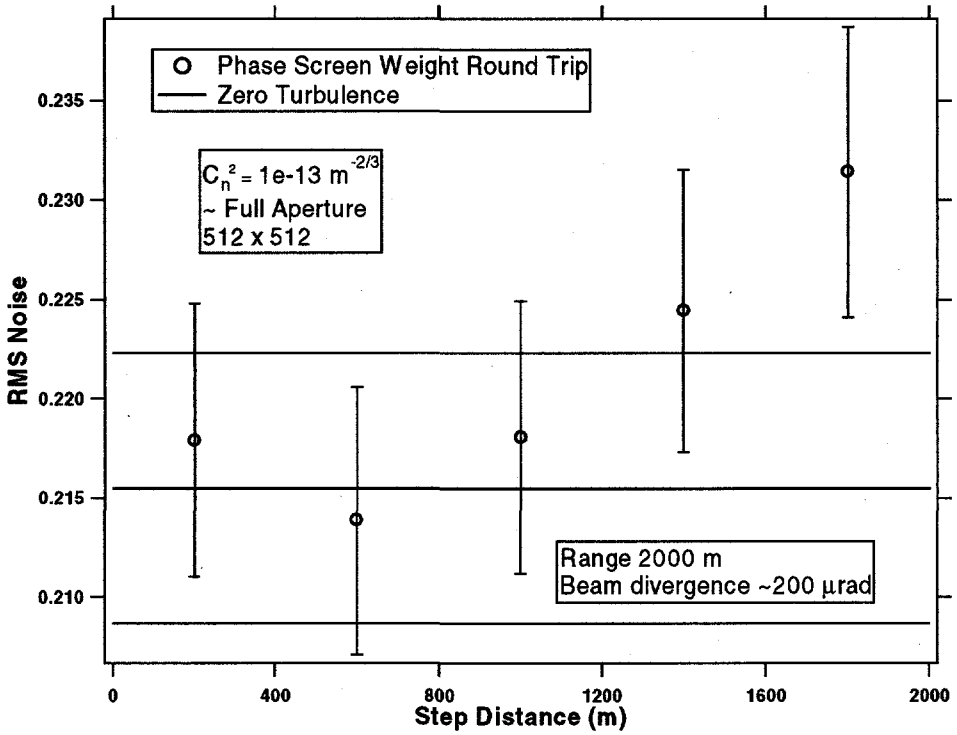

Figure 9. The effect of outgoing/return weighting of turbulence along the propagation path on the normalized standard deviation of intensity or RMS noise. The solid lines depict the mean and standard deviation for the vacuum case (Zero Turbulence) as in Figure 7. The circles (Phase Screen Weight Round Trip) indicate the case in which turbulence exists on the outgoing and return portions of only one propagation step (400 m).

7. REFERENCES

[1] D.H. Nelson, R.R. Petrin, E.P. MacKerrow, M.J. Schmitt, C.R. Quick, A. Zardecki, W.M. Porch, M.C. Whitehead and D.L. Walters, "Wave optics simulation of atmospheric turbulence and reflective speckle effects in CO_2 differential absorption LIDAR (DIAL)," *Airborne Laser Advanced Technology*, **3381**, 147-158, SPIE, Bellingham, WA (1998).

[2] D.H. Nelson, D.L. Walters, E.P. MacKerrow, M.J. Schmitt, C.R. Quick, W.M. Porch and R.R. Petrin, "Wave optics simulation of atmospheric turbulence and reflective speckle effects in CO_2 lidar," to be submitted to Applied Optics.

[3] J.F. Holmes, "Speckle propagation through turbulence: its characteristics and effects," *Proc. SPIE*, **410**, 89-97 (1983).

[4] M.V. Klein and T.E. Furtak, *Optics*, John Wiley & Sons, New York, 1986.

[5] J.W. Goodman, *Introduction to Fourier Optics* (McGraw-Hill, New York, 1968).

[6] D. L. Knepp, "Multiple phase-screen calculation of the temporal behavior of stochastic waves," *Proc. IEEE* **71**, 722-737 (1983).

[7] C.A. Davis and D.L. Walters, "Atmospheric inner-scale effects on normalized irradiance variance," *Appl. Opt*, **33**, 8406-8411 (1994).

[8] R.R. Beland, "Propagation through atmospheric turbulence," *The Infrared Electro-optical Systems Handbook*, Vol. 2, SPIE, Bellingham, WA, 157-232, 1993.

[9] J.M. Martin and S.M. Flatté, "Simulation of point-source scintillation through three-dimensional random media," *J. Opt. Soc. Am. A*, **7**, 838-847 (1990).

[10] J.M. Martin and S.M. Flatté, "Intensity images and statistics from numerical simulation of wave propagation in 3-D random media," *Appl. Opt*, **27**, 2111-2126 (1988).

[11] R.E. Hufnagel, "Propagation through atmospheric turbulence," *The Infrared Handbook*, Chapter 6, Environmental Research Institute of Michigan, Ann Arbor, MI, 1985.

[12] J.W. Goodman, "Statistical properties of laser speckle patterns," *Laser Speckle and Related Phenomena*, 2nd ed,. J. Dainty, Ed., Springer-Verlag, New York, 1984.

[13] E.P. MacKerrow and M.J. Schmitt, "Measurement of integrated speckle statistics for CO_2 lidar returns from a moving, nonuniform, hard target," *Appl. Opt*, **36**, 6921-6937 (1997).

[14] T. Wang, G.R. Ochs and S.F. Clifford, "A saturation-resistant optical scintillometer to measure C_n^2," *J. Opt. Soc. Am.*, **68**, 334-338 (1978).